Eur. Phys. J. A (2014) **50**: 111
DOI 10.1140/epja/i2014-14111-1

THE EUROPEAN PHYSICAL JOURNAL A

Letter

Heavy hybrid stars from multi-quark interactions

Sanjin Benić[a]

Department of Physics, Faculty of Science, University of Zagreb, P.O.B. 331, HR-10002 Zagreb, Croatia

Received: 22 June 2014
Published online: 14 July 2014

Communicated by D. Blaschke

Abstract. We explore the possibility of obtaining heavy hybrid stars within the framework of the two flavor Nambu–Jona-Lasinio model that includes 8-quark interactions in the scalar and in the vector channel. The main impact of the 8-quark scalar channel is to reduce the onset of quark matter, while the 8-quark vector channel acts to stiffen the equation of state at high densities. Within the parameter space where the 4-quark vector channel is small, and the 8-quark vector channel sizeable, stable stars with masses of $2\,M_\odot$ and above are found to hold quark matter in their cores.

1 Introduction

One of the most severe constraints of the equation of state (EoS) of QCD at extreme densities comes from the recent $2M_\odot$ mass determinations of PSR J1614-2230 [1] and PSR J0348-0432 [2] having important consequences for the existence of quark matter in compact stars [3–6].

In this work we assume compact stars are the so-called hybrid stars, composed of a nuclear mantle and a quark core. In order to obtain heavy hybrids stars, quark matter EoS should be stiff, with a low onset [7]. This can be achieved in the MIT bag model by perturbative corrections to the EoS and small bag pressures [8], while within the Nambu–Jona-Lasinio (NJL) model large vector channel is used for stiffness [9], while shift in the vacuum energy [10,11] or introduction of superconductivity ensures low onset [12]. An influence on the maximum mass is expected by the nature of the phase transition itself [13–15].

We propose an alternative scenario by taking into account the fact that NJL is a non-renormalizable effective model, valid up to some scale Λ. As we approach this scale, say by increasing the chemical potential, higher-dimensional operators should become important. It has been pointed out [16,17] that including higher scalar interactions can reduce the critical temperature in the NJL model, bringing it in closer agreement with lattice results at finite temperature [18]. For further work on higher-dimensional operators in the context of the NJL model see [19–25].

Our aim is to make an initial study of the effect of multiquark interactions on occurrence of quark matter in heavy stars. In this work we will use the NJL model parametrization of ref. [18] where the critical temperature at zero chemical potential is fitted to lattice QCD. In addition, we will also introduce the 8-quark vector channel, as a natural candidate for playing a relevant role at large densities reached in the cores of compact stars.

Our main results are that with scalar 8-quark interactions provided by ref. [18] we are able to obtain stable hybrid stars with small vector coupling in the 4-quark and zero vector coupling in the 8-quark channel. Second, we demonstrate that the mass of the star can be increased up to and above $2M_\odot$ with the 8-quark vector interaction, while still keeping the 4-quark vector interaction low.

2 NJL model with 8-quark interactions

We work within the framework of a $N_f = 2$ NJL model defined as follows:

$$\mathcal{L} = \bar{q}(i\,\partial\!\!\!/ - m)q + \mu_q \bar{q}\gamma^0 q + \mathcal{L}_4 + \mathcal{L}_8, \tag{1}$$

where μ_q is the quark chemical potential and m is the current mass. The interaction terms are

$$\mathcal{L}_4 = \frac{g_{20}}{\Lambda^2}\left[(\bar{q}q)^2 + (\bar{q}i\gamma_5\boldsymbol{\tau}q)^2\right] - \frac{g_{02}}{\Lambda^2}(\bar{q}\gamma_\mu q)^2, \tag{2}$$

$$\mathcal{L}_8 = \frac{g_{40}}{\Lambda^8}\left[(\bar{q}q)^2 + (\bar{q}i\gamma_5\boldsymbol{\tau}q)^2\right]^2 - \frac{g_{04}}{\Lambda^8}(\bar{q}\gamma_\mu q)^4 - \frac{g_{22}}{\Lambda^8}(\bar{q}\gamma_\mu q)^2\left[(\bar{q}q)^2 + (\bar{q}i\gamma_5\boldsymbol{\tau}q)^2\right], \tag{3}$$

where Λ is the model cutoff. The Lagrangian (1) may be motivated by the large N_c counting: while the 4-quark couplings scale as $1/N_c$, the 8-quark couplings scale as $1/N_c^3$ [26].

[a] e-mail: sanjinb@phy.hr

In the mean-field approximation the Lagrangian becomes

$$\mathcal{L}_{\rm MF} = \bar{q}(i\ \partial\!\!\!/ - M)q + \tilde{\mu}_q \bar{q}\gamma^0 q - U, \tag{4}$$

where

$$M = m + 2\frac{g_{20}}{\Lambda^2}\langle\bar{q}q\rangle + 4\frac{g_{40}}{\Lambda^8}\langle\bar{q}q\rangle^3 - 2\frac{g_{22}}{\Lambda^8}\langle\bar{q}q\rangle\langle q^\dagger q\rangle^2, \tag{5}$$

$$\tilde{\mu}_q = \mu_q - 2\frac{g_{02}}{\Lambda^2}\langle q^\dagger q\rangle - 4\frac{g_{04}}{\Lambda^8}\langle q^\dagger q\rangle^3 - 2\frac{g_{22}}{\Lambda^8}\langle\bar{q}q\rangle^2\langle q^\dagger q\rangle, \tag{6}$$

and the classical potential

$$U = \frac{g_{20}}{\Lambda^2}\langle\bar{q}q\rangle^2 + 3\frac{g_{40}}{\Lambda^8}\langle\bar{q}q\rangle^4 - 3\frac{g_{22}}{\Lambda^8}\langle\bar{q}q\rangle^2\langle q^\dagger q\rangle^2 - \frac{g_{02}}{\Lambda^2}\langle q^\dagger q\rangle^2 - 3\frac{g_{04}}{\Lambda^8}\langle q^\dagger q\rangle^4. \tag{7}$$

Integrating out the quark degrees of freedom, the full thermodynamic potential takes the following form:

$$\Omega = U - 2N_f N_c \int \frac{\mathrm{d}^3 p}{(2\pi)^3}\Big\{E + T\log\left[1 + e^{-\beta(E-\tilde{\mu}_q)}\right] + T\log\left[1 + e^{-\beta(E+\tilde{\mu}_q)}\right]\Big\} + \Omega_0, \tag{8}$$

where $E = \sqrt{\mathbf{p}^2 + M^2}$ and $\beta = 1/T$ and where Ω_0 ensures zero pressure in the vacuum. The model is solved by minimizing the thermodynamic potential with respect to the mean fields $X = \langle\bar{q}q\rangle, \langle q^\dagger q\rangle$, *i.e.*

$$\frac{\partial\Omega}{\partial X} = 0. \tag{9}$$

In this work we use the parameter set of ref. [18] $g_{20} = 1.864$, $g_{40} = 11.435$, $m = 5.5\,\mathrm{MeV}$ $\Lambda = 631.5\,\mathrm{MeV}$. The vector channel strengths are treated as free parameters, quantified by

$$\eta_2 = \frac{g_{02}}{g_{20}}, \qquad \eta_4 = \frac{g_{04}}{g_{40}}. \tag{10}$$

We are interested in a particular region of the vector channel couplings where the g_{02} coupling is kept small, while g_{04} is increased. The reason behind our choice is as following. Since heavy hybrid stars require a stiff EoS, a repulsive vector coupling should be present. As the vector coupling renormalizes the chemical potential, it delays the onset of quark matter. This leads to a scenario where the hadronic mantle becomes too large for the pressure in the quark core to be able to hold the star against gravitational collapse. Therefore, the appearance of quark matter in such a scenario usually makes the star unstable. An attractive channel like *e.g.*, superconductivity needs to be invoked in order to lower the onset [12]. We point out that an alternative microscopic picture is possible with multiquark interactions: whereas stiffening of the EoS is provided by the 8-quark vector channel interaction, lowering of the onset is accomplished by introducing a sizeable 8-quark scalar channel interaction and keeping the 4-quark vector channel interaction small.

Our choice of the phenomenologically interesting parameter space will have an effect of stiffening the quark matter at higher densities, while at the same time keeping the transition density low. Due to this restriction we will also put $g_{22} = 0$ by hand. Namely, the operator controlled by the size of g_{22} can be important at moderate μ_q only if the vector mean field is sizeable, which will not be the case for the parameter region of small g_{02} in which we are interested in. In addition, it will not be important at high μ_q since there the scalar mean field is zero.

3 Equation of state

By evaluating the full thermodynamical potential (8) at the minimum, we obtain the quark matter EoS as $p_q = -\Omega$. The quark number density n_q and energy density ϵ_q are defined as follows:

$$n_q = -\frac{\partial p_q}{\partial \mu_q}, \qquad \epsilon_q = -p_q + n_q\mu_q. \tag{11}$$

Beta equilibrium is taken into account by the weak processes $d \to u + e^- + \bar{\nu}_e$, $\mu^- \to e^- + \nu_\mu + \bar{\nu}_e$, implying $\mu_u = \mu_d + \mu_e$, $\mu_\mu = \mu_e$, where the neutrino chemical potential is set to zero. Finally, the baryon chemical potential, and the baryon density are $\mu_B = 3\mu_q = 2\mu_d + \mu_u$ and $n_B = n_q/3$, respectively.

For the nuclear matter we choose the DD2 EoS [27,28]. The transition from nuclear to quark matter is provided by the traditional Maxwell construction. Therefore, the EoS is obtained by requiring local charge neutrality. The full pressure in the quark phase takes into account the contribution of electrons and muons

$$p(\mu_q) = p_u(\mu_u) + p_d(\mu_d) + p_e(\mu_e) + p_\mu(\mu_\mu), \tag{12}$$

where $p_{e,\mu}$ is the pressure of a free electron (muon) gas. We emphasize that the Maxwell construction is merely the limit of large surface tension at the quark-hadron interface in a more elaborate approach that takes into account finite-size effects, see [29]. The following results ultimately depend also on the choice of the construction of the phase transition.

The hybrid EoS are given in fig. 1 for $\eta_2 = 0.05$ and a range of η_4. Owing to 8-quark scalar interactions, and small 4-quark vector interactions, onset of quark matter is rather low: for $\eta_2 = 0.05$ and $\eta_4 = 0.0$ it is around $\epsilon \simeq 500\,\mathrm{MeV/fm^3}$. Even a drastic increase of η_4 has barely any influence on the onset: this is only natural, since there is extra suppression due to high dimensionality of the corresponding operator.

The influence of η_4 is best seen by inspecting the speed of sound: while small or almost vanishing vector interactions yield the relativistic value $c_s^2 \simeq 1/3$, the speed of sound significantly increases with ϵ already for $\eta_4 = 1.0$, see right panels of fig. 1. This gradual stiffening of the EoS can also be seen as a microscopic mechanism of a postulated scenario of a medium-dependent parameter η_2 [30], which is able to provide a very stiff quark EoS [7]. Assuming that the vector mean field is given by the density of

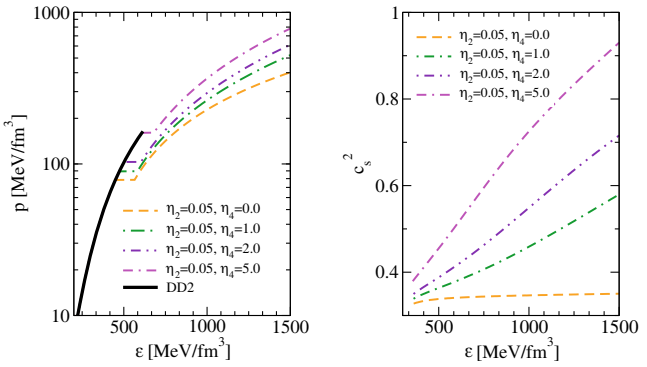

Fig. 1. (Color online) On the left panel we show the EoS of hybrid matter. Thick black curve is the hadronic contribution. Flat region corresponds to Maxwell construction. We fix $\eta_2 = 0.05$. Quark matter curves are denoted as following: the orange, dashed line accounts for $\eta_4 = 0.0$, dash-dotted, green line for $\eta_4 = 1.0$, dash-double-dotted, indigo line for $\eta_4 = 2.0$ and double-dash-dotted, magenta line for $\eta_4 = 5.0$. Right panel shows the speed of sound of quark matter with the same labeling.

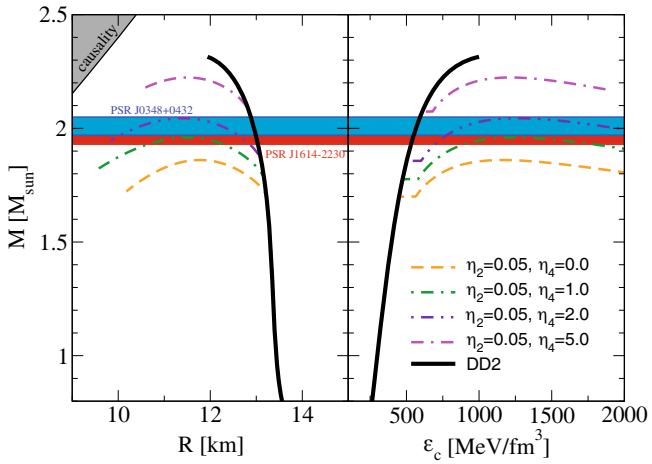

Fig. 2. (Color online) Left panel shows the M-R and the right panel the M-ϵ_c diagram of compact star solutions within the model. We fix $\eta_2 = 0.05$. The detachment from the hadronic branch given by the thick, black curve and the maximum mass depends on η_4. Hybrid star branches appear in the same line styles as the corresponding EoS in fig. 1. Hatched regions mark experimental constraints from two heaviest sources, lower, red is [1], while higher, blue is [2].

massless fermions, an approximative expansion in g_{02} and g_{04} for the speed of sound $c_s^2 = \partial p/\partial\epsilon$ as a function of the quark chemical potential can be shown to hold

$$c_s^2 \simeq \frac{1}{3} + \frac{32 g_{02}}{6\pi^2}\frac{\mu_q^2}{\Lambda^2} + \frac{512 g_{02}^2}{4\pi^4}\frac{\mu_q^4}{\Lambda^4} + \frac{75776 g_{02}^3}{24\pi^6}\frac{\mu_q^6}{\Lambda^6} + \frac{3768320 g_{02}^4}{48\pi^8}\frac{\mu_q^8}{\Lambda^8} + \frac{8192 g_{04}}{48\pi^8}\frac{\mu_q^8}{\Lambda^8}, \quad (13)$$

illustrating that the g_{04} term starts to be important only at higher chemical potentials. While the 4-quark vector interaction respects causality, strong 8-quark vector interaction may violate the causal limit, see ref. [31] for an explicit example in the nucleonic NJL model. This is the reason why the EoS with $\eta_4 = 5.0$ turns acausal already at $\epsilon \sim 2000\,\mathrm{MeV/fm^3}$. In addition, for such high densities, the quark chemical potential is approaching Λ where the model should not be trusted anymore. Therefore, results obtained for this extreme scenario are given for illustrative purposes.

4 Hybrid stars

The static, spherically symmetric stars are obtained as solutions of the Tolman-Oppenheimer-Volkoff (TOV) equations for the EoS shown in the previous section. In fig. 2 we display the resulting mass-radius and mass-central energy density diagrams for $\eta_2 = 0.05$.

Due to the early onset of quark matter, in fig. 2 we are able to obtain stable stars with pure quark matter in their cores even for very small vector coupling. Such a scenario is not easy to achieve in the NJL model with only fourth-order scalar and vector operators [12,32], see however [11]. The strong vector interaction increases the speed of sound and makes quark matter stiff, but at the same time it appears at too high energy densities. The higher-dimensional vector operator stiffens the EoS and without influencing the onset significantly, gives a mechanism for $2\,M_\odot$ hybrid stars, see fig. 2. In order to cover the present experimental window provided by PSR J1614-2230 and PSR J0348-0432 we have found that values η_4 up to $\eta_4 \sim 2.0$ are sufficient. The extreme case with $\eta_4 = 5.0$ leads to a significant increase in the mass, yielding $M \sim 2.25\,M_\odot$.

5 Conclusions

Observing heavy compact stars offers a promising perspective on constraining the cold, dense EoS beyond saturation density. A compelling discrimination of many possible scenarios of dense matter will be possible once precise measurements of also star radii become available [33]. The data of both masses and radii will enable Bayesian inversion of the TOV equation leading to the EoS [34].

We have studied one possible scenario where multi-quark interactions coming from higher-dimensional operators in the NJL model might play an important role at large densities. A sizeable 8-quark scalar channel is introduced in order to achieve a low onset. With a small 4-quark vector coupling onset is still low, while the relatively large 8-quark coupling is used to gradually stiffen the EoS at high densities. Within this parameter space we were able to fulfill and go beyond the $2M_\odot$ constraint.

The scenario of small 4-quark vector coupling is in accordance with the results of ref. [35,36], but a more thorough study is needed to reveal how would the introduction of the 8-quark vector coupling influence their results. In addition, we stress that the consensus concerning the status of vector interactions in quark matter is yet to be reached in the community, as some other studies [18,37–39] advocate a different scenario where the

4-quark vector coupling is sizeable. Using the results from the lattice QCD measurements at finite T [40–42] and at imaginary chemical potential [43] a more thorough study of the model presented here is needed to achieve better constraints on the three vector channel couplings, and to investigate the consequences at large densities. Finally, it remains to be explored what can such a setup say about the existence of strangeness in compact stars.

The author acknowledges illuminating discussions with D. Blaschke and thanks D.E. Alvarez-Castillo for help with the TOV code. The author also thanks the Yukawa Institute for Theoretical Physics, Kyoto University, where part of this work was performed during the YITP-T-13-05 workshop on "New Frontiers in QCD". This work is supported by the MIAU project of the Croatian Science Foundation and by the the COST Action MP1304 NewCompStar.

References

1. P. Demorest *et al.*, Nature **467**, 1081 (2010).
2. J. Antoniadis *et al.*, Science **340**, 6131 (2013).
3. F. Ozel, Nature **441**, 1115 (2006).
4. T. Klahn, D. Blaschke, F. Sandin, C. Fuchs, A. Faessler, H. Grigorian, G. Ropke, J. Trumper, Phys. Lett. B **654**, 170 (2007).
5. M. Alford, D. Blaschke, A. Drago, T. Klahn, G. Pagliara, J. Schaffner-Bielich, Nature **445**, E7 (2007).
6. J.M. Lattimer, M. Prakash, *What a Two Solar Mass Neutron Star Really Means*, in *From Nuclei to Stars* (World Scientific, 2011) doi: 10.1142/9789814329880_0012.
7. M.G. Alford, S. Han, M. Prakash, Phys. Rev. D **88**, 083013 (2013).
8. S. Weissenborn, I. Sagert, G. Pagliara, M. Hempel, J. Schaffner-Bielich, Astrophys. J. **740**, L14 (2011).
9. M. Hanauske, L.M. Satarov, I.N. Mishustin, H. Stoecker, W. Greiner, Phys. Rev. D **64**, 043005 (2001).
10. G. Pagliara, J. Schaffner-Bielich, Phys. Rev. D **77**, 063004 (2008).
11. C.H. Lenzi, G. Lugones,, Astrophys. J. **759**, 57 (2012).
12. T. Klahn, D.B. Blaschke, R. Łastowiecki, Phys. Rev. D **88**, 085001 (2013).
13. N. Yasutake, T. Noda, H. Sotani, T. Maruyama, T. Tatsumi, arXiv:1208.0427 [astro-ph.HE].
14. K. Masuda, T. Hatsuda, T. Takatsuka, Prog. Theor. Exp. Phys. **2013**, 073D01 (2013).
15. D.E. Alvarez-Castillo, S. Benic, D. Blaschke, R. Lastowiecki, Acta Phys. Pol. B **7**, 203 (2014).
16. A.A. Osipov, B. Hiller, J. Moreira, A.H. Blin, J. da Providencia, Phys. Lett. B **646**, 91 (2007).
17. A.A. Osipov, B. Hiller, J. Moreira, A.H. Blin, Phys. Lett. B **659**, 270 (2008).
18. Y. Sakai, K. Kashiwa, H. Kouno, M. Matsuzaki, M. Yahiro, Phys. Rev. D **79**, 096001 (2009).
19. T. Lee, Y.-s. Oh, Phys. Lett. B **475**, 207 (2000).
20. I.N. Mishustin, L.M. Satarov, W. Greiner, Phys. Rep. **391**, 363 (2004).
21. K. Kashiwa, H. Kouno, T. Sakaguchi, M. Matsuzaki, M. Yahiro, Phys. Lett. B **647**, 446 (2007).
22. R. Huguet, J.C. Caillon, J. Labarsouque, Nucl. Phys. A **781**, 448 (2007).
23. K. Kashiwa, M. Matsuzaki, H. Kouno, M. Yahiro, Phys. Lett. B **657**, 2007 (143).
24. R. Gatto, M. Ruggieri, Phys. Rev. D **83**, 2011 (034016).
25. A. Ohnishi, H. Ueda, T.Z. Nakano, M. Ruggieri, K. Sumiyoshi, Phys. Lett. B **704**, 284 (2011).
26. R. Alkofer, I. Zahed, Phys. Lett. B **238**, 149 (1990).
27. S. Typel, H.H. Wolter, Nucl. Phys. A **656**, 331 (1999).
28. S. Typel, G. Ropke, T. Klahn, D. Blaschke, H.H. Wolter, Phys. Rev. C **81**, 015803 (2010).
29. T. Maruyama, S. Chiba, H.-J. Schulze, T. Tatsumi, Phys. Rev. D **76**, 123015 (2007).
30. D. Blaschke, D.E. Alvarez-Castillo, S. Benic, PoS CPOD **2013**, 063 (2013).
31. T.J. Burvenich, D.G. Madland, Nucl. Phys. A **729**, 769 (2003).
32. M. Orsaria, H. Rodrigues, F. Weber, G.A. Contrera, Phys. Rev. C **89**, 015806 (2014).
33. M.C. Miller, arXiv:1312.0029 [astro-ph.HE].
34. A.W. Steiner, J.M. Lattimer, E.F. Brown, Astrophys. J. **765**, L5 (2013).
35. J. Steinheimer, S. Schramm, Phys. Lett. B **696**, 257 (2011).
36. S. Schramm, V. Dexheimer, R. Negreiros, T. Schürhoff, J. Steinheimer, arXiv:1306.0989 [astro-ph.SR].
37. N.M. Bratovic, T. Hatsuda, W. Weise, Phys. Lett. B **719**, 131 (2013).
38. G.A. Contrera, A.G. Grunfeld, D.B. Blaschke, Phys. Part. Nucl. Lett. **11**, 342 (2014).
39. J. Sugano, J. Takahashi, M. Ishii, H. Kouno, M. Yahiro, arXiv:1405.0103 [hep-ph].
40. M. Cheng, P. Hendge, C. Jung, F. Karsch, O. Kaczmarek, E. Laermann, R.D. Mawhinney, C. Miao *et al.*, Phys. Rev. D **79**, 074505 (2009).
41. O. Kaczmarek, F. Karsch, E. Laermann, C. Miao, S. Mukherjee, P. Petreczky, C. Schmidt, W. Soeldner *et al.*, Phys. Rev. D **83**, 014504 (2011).
42. A. Bazavov, T. Bhattacharya, M. Cheng, C. DeTar, H.T. Ding, S. Gottlieb, R. Gupta, P. Hegde *et al.*, Phys. Rev. D **85**, 054503 (2012).
43. P. de Forcrand, O. Philipsen, Nucl. Phys. B **642**, 290 (2002).